

ONE DIMENSIONAL NETWORK MODEL FOR A REVERSE FLOW COMBUSTOR

Gökhan Varol* and Gürkan Sarıkaya†

Istanbul Technical University, Istanbul, 34469, Turkey

Onur Tuncer‡

Istanbul Technical University, Istanbul, 34469, Turkey

In this study, a one-dimensional empirical network code was developed for the preliminary design of a reverse flow combustor, which was intended to be used in a 1000 hp turbo-shaft helicopter engine. Network code is able to predict critical design features such as discharge coefficients at each hole set, mass flow rate distributions across the swirler, cooling devices and dilution holes, overall pressure drop across the combustor, liner wall and gas temperatures along the combustor and pollutant emissions at the exit of the combustor. By these means, many design alternatives can be scanned rapidly in early stages of design. Results are presented for a particular combustor geometry operating at idle, cruise and take-off conditions based on the cycle analysis of a turbo-shaft engine design which is intended for light duty helicopter missions. Calculated flow distributions and discharge coefficients were compared with isothermal numerical simulations and reasonably good agreement was achieved for the non-reacting case. On the other hand, liner temperatures for three operating conditions obtained from the network code were examined to see whether the liner temperatures were suitable for liner material and the obtained results showed that this particular design raises doubts when viewed from the predicted high liner temperatures.

Nomenclature

A	Area [m^2]
A/F	Air/fuel ratio
C/H	Carbon to hydrogen ratio
C_d	Discharge Coefficient
C_1	Internal Convection [W]
C_2	Convection to annulus [W]
C_3	External Convection [W]
D_h	Hydraulic diameter [m]
F/A	Fuel/air ratio
K	Loss coefficient
K_{1-2}	Conduction through liner wall [W]
K_{2-3}	Conduction through liner wall [W]
L_u	Luminosity factor
P	Total pressure [Pa]
P_i	Total pressure upstream of hole [Pa]
P_w	Wetted perimeter [m]
R	Radiation [W]
T	Temperature [K]

*Graduate Student, Aeronautical Engineering, ITU UUBF Maslak Istanbul 34469 Turkey, AIAA Member

†Research Assistant, Aeronautical Engineering, ITU UUBF Maslak Istanbul 34469 Turkey, AIAA Member

‡Assoc.Prof.Dr.Onur Tuncer, Aeronautical Engineering, ITU UUBF Maslak Istanbul 34469 Turkey, AIAA Member, Corresponding Author

$T_{w,ad}$	Gas temperature at the combustor liner wall [K]
ΔT	Temperature rise [K]
Q	Volume flow rate [m^3/s]
V	Velocity [m/s]
V_c	Combustion volume [m^3]
l_b	Beam length [m]
k	Conductivity [W/mK]
m	Mass flow rate [kg/s]
p_i	Static pressure upstream of hole [Pa]
p_j	Static pressure downstream of hole [Pa]
t_w	Liner wall thickness [m]

Symbols

ϕ	Equivalence ratio
ρ	Density [kg/m^3]
η_c	Combustion efficiency
η_f	Film-cooling efficiency
ε_g	Gas emissivity
ε_w	Wall emissivity
σ	Stefan Boltzmann constant
μ	Viscosity [kg/ms]
α	Mass flow ratio
φ	(Mass flow ratio)/(Area ratio)

Subscripts

a	Air
an	Annulus
c	Casing
g	Gas
st	Stoichiometric
h	Hole/Hub
L	Combustor liner
max	Maximum
out	Zone outlet
w_1	Inner liner wall
w_2	Outer liner wall
$zone$	Recirculation, primary, secondary, dilution zone
PZ	Primary zone
SZ	Secondary zone
1	Inner liner wall
3	Combustor inlet
4	Combustor outlet

I. Introduction

Gas turbine combustor design and development is a process that is carried out using various methods such as empirical correlations, numerical investigations and experimental studies. The main purpose of these methods is to predict mass flow distributions through liner holes, overall pressure loss, combustion efficiency, temperature distribution through the liner and inside the flame tube and pollutant emissions. However, each method has some advantages and disadvantages relative to the others. Despite the fact that the empirical/analytical method provides valuable data in less time, the accuracy is limited by the sub-models predicting turbulence, combustion and heat transfer.¹

By means of increasing the processor speed, numerical methods such as CFD (Computational Fluid Dynamics) became an attractive alternative. This approach has its advantages in predicting the complex

reacting flow domain in the entire volume of combustor, but when fast results are required for quick design evaluation then CFD has disadvantages in terms of computational time.¹ Thus, only after the preliminary design process is complete does CFD analysis become necessary for the detailed investigation of the three dimensional reacting flow within the combustor. On the other hand, experiments are also an essential part of the design process in spite of its difficulty and expensiveness. Therefore, empirical and numerical methods are needed to reduce experimental tests by determining initial design data such as total pressure losses through the combustion chamber and flow distributions across the combustor volume.

Knight and Walker conducted a pioneering analysis to determine pressure losses for combustor features to define flow distributions across the combustor holes at the preliminary design stage.² With the development of computers, one dimensional analysis has become a valuable tool in terms of lower computational time requirements. Samuel developed a one dimensional analytical method to predict pressure distribution and mass flow rates for annular and can annular combustors³ and a similar approach for reverse flow combustors was developed by Joubert and Hattingh.⁴ However, these approaches are not suitable for complex geometries.

On the other hand, the one dimensional network model overcomes this challenge with the same computation time for complicated geometries. The network model solves the conservation equations on a one dimensional node array and uses empirical correlations to predict combustion efficiency, discharge coefficients etc. These empirical models provide design engineers with reduced development time and optimize the preliminary design data for different combustor geometries.

Network models can utilize three different methods such as node methods, loop solver methods, and element methods. The first two methods require initial mass pressure for each element or initial mass flow rate for each node to satisfy continuity for each node while element solution methods do not need to satisfy the continuity equation.⁵ Greyvanstein and Laurie developed a network algorithm for compressible flow in pipes and integrated the SIMPLE algorithm, which is a type of node method, into their network model.⁷ Stuttford described a calculation method to determine the pressure drop and incompressible flow distributions throughout the combustor by using continuity equations and pressure drop relations, and incorporating heat transfer processes between the nodes.⁷ Note that complex combustor geometries commonly include features like cooling rings, dilution jet ports, swirl vanes etc. Flow and heat transfer processes for these features need to modeled based on experiments or theory. Thereafter, Gouws developed a MATLAB based network solver that is empirically based and solves the incompressible flow for tubular and can annular through-flow combustors and tested it for T56 combustor geometry l.⁸

A solid model of the reverse flow combustor studied here is provided in Figure 1. These combustors are preferred in helicopter engines since they enable more compact engine design. However, due to reversal of the flow direction there is a pressure drop penalty.

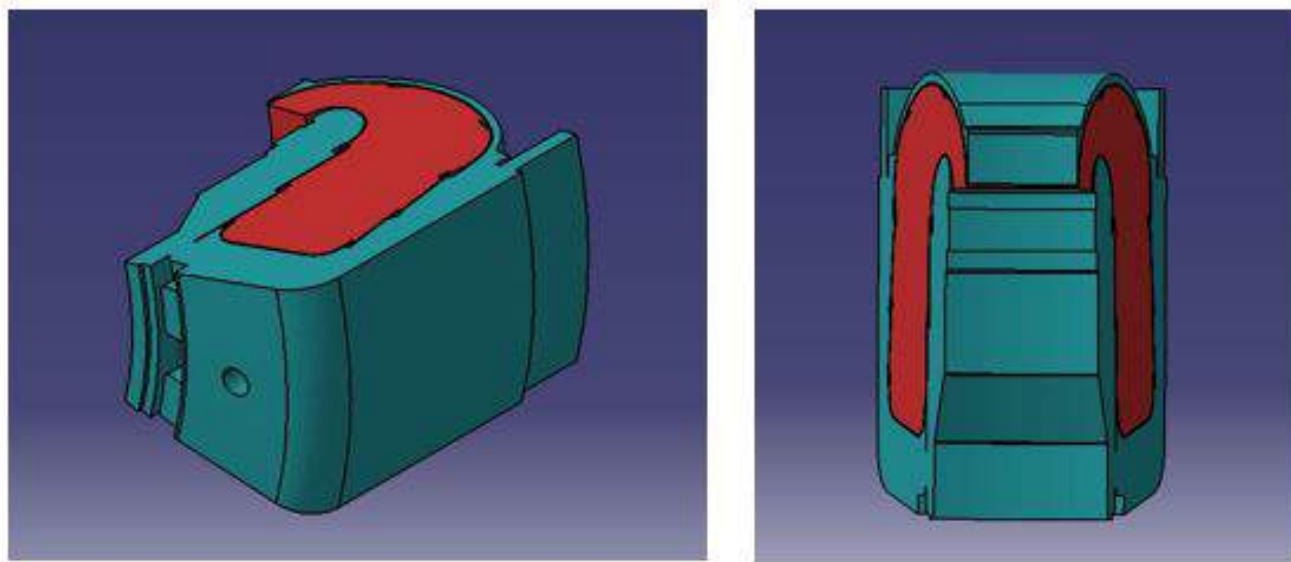


Figure 1: Solid model of the reverse flow combustor (Red color indicates flametube, green color indicates inlet flow)

In this study, this code was modified for 1/13 section of the reverse flow annular combustor. Because of the non-symmetrical liner geometry and use of the one dimensional flow calculation method, the combustor is divided into two equal adjoint regions that are described as the inner and outer region as shown in Figure 2. Calculations were made for the two regions and results were combined for the entire volume by using mass weighted average calculation.

The combustion zone is divided into four sections, namely re-circulation zone, primary zone, secondary zone and dilution zone, respectively. Combustor liner consists of three film cooling device sets and two jet hole sets as illustrated in Figure 2.

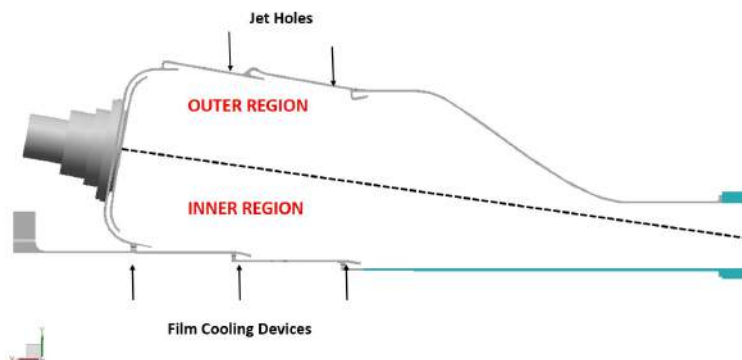


Figure 2: Planar Section View of Reverse Flow Combustor

II. Mathematical Model

The one-dimensional network solver is able to predict mass-flow distributions, gas and liner temperatures and pressure drop across the combustion chamber.

A. Network Layout for the Combustor

Figure 4 shows the network layout for reverse flow annular combustion chamber. The layout comprises a number of elements that are linked by nodes. The circles and squares represent the network node and flow elements, respectively. Empirical correlations are handled to describe the flow through the element and overall governing equations are solved within nodes. The overall governing equations are the continuity equations and a pressure drop/flow rate relationship that is applied at every node and elements in the network model, respectively.⁷ Figure 3 shows a simple network section. The continuity equation can be described as,

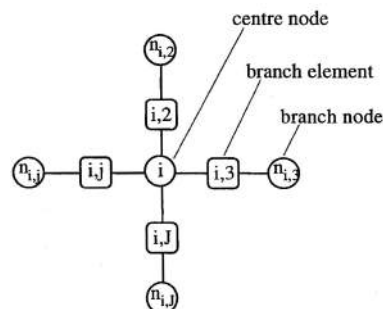


Figure 3: Network Array⁷

$$\sum_{j=1}^J \rho_{i,j} Q_{i,j} s_{i,j} = -d_i \quad i = 1, 2, \dots, J \quad (1)$$

and pressure drop/flow rate relationship defined as,

$$\Delta P_{i,j} = P_{n_{i,j}} - P_i = s_{i,j} H_{i,j} g_{i,j} f_{i,j} \quad (2)$$

The $s_{i,j}$ term in Eq. 1 and Eq. 2 represents the flow direction as positive direction if $s_{i,j} = 1$ and negative direction if $s_{i,j} = -1$.

Network models have various types of geometric features for flow elements. The DC elements, which represent a duct with area change, model the flow within the flame tube and the annulus section. These elements are related to the area changes across the combustor and inlet conditions. Also, the annulus flow field and the flame tube flow field are connected with this type of element. The RL elements, which represent the restriction with loss coefficient, apply to model the swirler. The loss coefficient of the swirler is known to solve the total pressure drop equation. The RD elements, which represent the restrictor with discharge coefficient, apply to model the swirler. The discharge coefficient of the swirler is known to solve the total pressure drop equation.

Computation procedure of the network model starts with defining an initial pressure value at each node and calculates density by using ideal gas equation. The predicted mass flow rate is then calculated by using

Eq. 2. The predictions are corrected by using the following relationships,

$$\begin{aligned} P &= P^* + P' \\ Q &= Q^* + Q' \\ \rho &= \rho^* + \rho' \end{aligned} \quad (3)$$

The * symbol refers to the predicted values and the ' symbol represents the correction data. The correction procedure presented by Greyvanstein and Laurie⁶ is applied to satisfy the governing equations. Thereafter, mass flow rates at each node are obtained with iteration process when the convergence is achieved.

The convective, conductive and radiative heat transfer elements are used for modeling the heat transfer process through the liner wall. The energy equation is satisfied by balancing the enthalpy for every node, thus the heat transfer process is described. The convection and radiation heat transfers are used to describe the heat transfer process from the combustion gas to the liner wall. Figure 5 shows the heat transfer process in a part of the combustor. In this figure, the black nodes are the fixed temperature nodes and they have fixed property values.

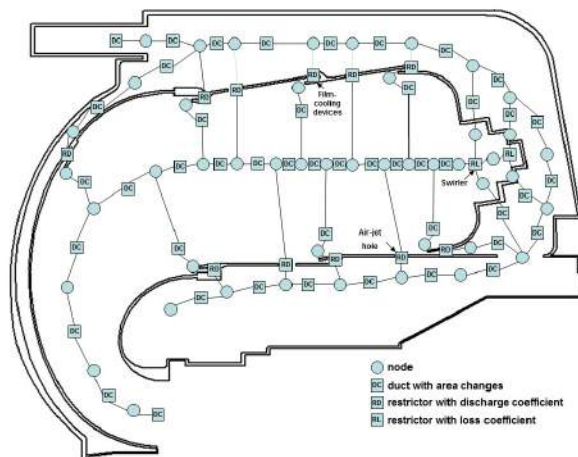


Figure 4: Flow network layout for a reverse flow combustor

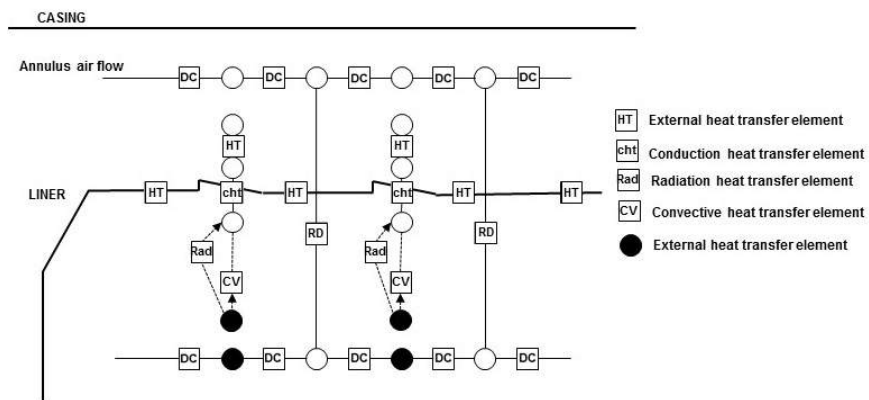


Figure 5: General heat transfer process network between hot gases and combustor liner⁸

B. Flow Calculations

For a preliminary one-dimensional design analysis, the empirical and analytical correlations can be used to predict the mass flow distributions across the combustor. The geometry of the combustor liner and pressure drop are factors that can affect the mass flows through the holes on the combustor liner. The Bernoulli equation is combined with the continuity equation to evaluate the empirical equation for incompressible flow.

$$m_h = C_d A_h (2\rho(P_1 - p_j))^{0.5} \quad (4)$$

The discharge coefficient is defined according to Eq. 5.

$$C_d = m_h / (\rho V_j A_h) \quad (5)$$

Norster⁹introduced a number of empirical correlations for the estimation of discharge coefficients of various hole features. These correlations are valid for plain and plunged holes; however the film cooling holes have different characteristics.

Plain holes:

$$C_d = \frac{1.25(K - 1)}{\sqrt{(4K^2 - K(2 - \alpha))^2}} \quad (6)$$

Plunged holes:

$$C_d = \frac{1.65(K - 1)}{\sqrt{(4K^2 - K(2 - \alpha))^2}} \quad (7)$$

K is the hole loss coefficient and α is the hole bleed ratio defined as the following equations;

$$K = 1 + 0.64(2\varphi^2 + \sqrt{\varphi^4 + 1.56\varphi^2(4\alpha - \alpha^2)}) \quad (8)$$

where;

Mass flow ratio:

$$\alpha = \frac{\dot{m}_h}{\dot{m}_{an}} \quad (9)$$

Hole area ratio:

$$A_r = \frac{A_{h,geom}}{A_{an}} \quad (10)$$

Mass flow ratio/area ratio:

$$\varphi = \frac{\alpha}{A_r} \quad (11)$$

The jet flow angle for plain and plunged holes can be expressed as a function of loss coefficient, K, as follows:

$$\sin\theta = \frac{1}{1.6C_d} \frac{(K - 1)}{K} \quad (12)$$

$$\sin\theta = \frac{1}{1.2C_d} \frac{(K - 1)}{K} \quad (13)$$

Using the above equations and correlations, pressure drop and mass flow rate distribution for each hole can be predicted with the following procedure:

- Use Eq. 4 to describe a relation between mass flow rate and pressure
- Presume an initial mass flow rate for each holes
- Using initial presumption, calculate discharge coefficient as follows

step 1: Calculate α from Eq. 9

step 2: Calculate A_r from Eq. 10

step 3: Calculate φ from Eq. 11

step 4: Calculate K with using Eq. 8

step 5: Use calculated K into Eq. 6 or Eq. 7 to determine discharge coefficient

- Calculate areal pressure drop along the liner
- Adjust mass flow rate in each hole by the calculated pressure drop
- Restart iteration with new mass flow rate and pressure drop until converges

C. Combustion Calculations

The combustion chamber is divided into four zones known as recirculation, primary, secondary and dilution zones. For the prediction of airflow within each zone, air flow mass fraction for each zone was assumed according to the following practice. The flow in re-circulation zone is the sum of all the flows coming from the swirler and half of the air coming from the first hole set. The flow in the primary zone is the sum of the remaining flow from the first hole set, and half of the air coming from the second and third hole set. The secondary zone includes half of the air coming from the second, third and fourth hole sets plus one third of the fifth hole set. The remaining air flow is used for the dilution zone. By using the total amount of air and stoichiometric air/fuel ratio of n-heptane, the equivalence ratio of each zone can be calculated. Olikara and Borman routine is utilized to predict the adiabatic flame temperature of n-heptane.¹⁰ The temperature rise (ΔT) can subsequently be obtained for each specific combustion zone using the Eq. 14.

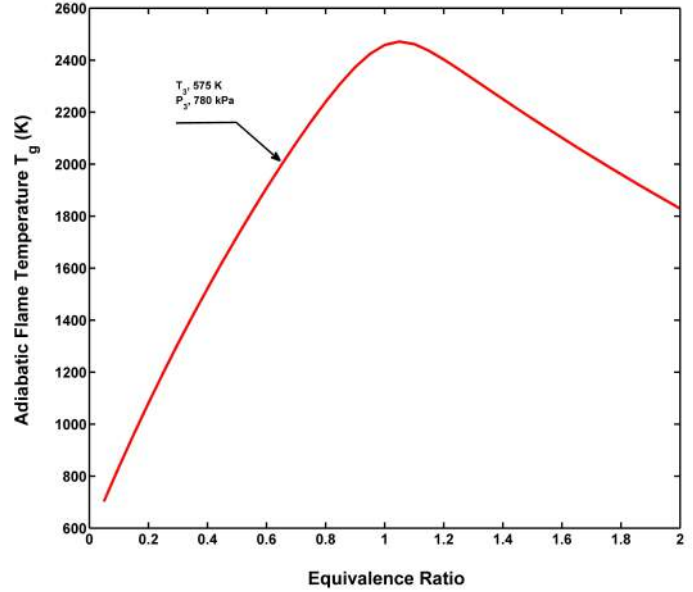


Figure 6: Adiabatic Flame Temperature Curve

$$\Delta T = T_g - T_3 \quad (14)$$

In this study, adiabatic flame temperature for n-heptane fuel which is shown in Figure 6.

For the prediction of gas temperature, combustion efficiency should be taken into account. Gosselin, Odgers and Kretschmer presented empirical correlation for the calculation of combustion efficiency in the recirculation, primary, secondary and dilution zones as expressed below.^{11,12}

The efficiency correlation for recirculation zone is,

$$\eta_{RZ} = 0.56 + 0.44 \tanh[1.5475 \times 10^{-3}(T_3 + 108 \ln(P_3) - 1863)] \quad (15)$$

The combustion efficiency for primary zone is,

$$\eta_{PZ} = 0.71 + 0.29 \tanh[1.5475 \times 10^{-3}(T_3 + 108 \ln(P_3) - 1863)] \quad (16)$$

For the secondary and dilution zones, this correlation estimates lower values than the primary zone. Therefore, combustion efficiencies were assumed to be 90

The maximum temperature in the re-circulation zone is calculated as follows:

$$T_{out,RZ} = T_3 + \eta_{RZ} \Delta T \quad (17)$$

Re-circulation zone can be approximated with a partially stirred reactor such that maximum temperature only occurs locally. For this reason, average outlet temperature is assumed as,

$$T_{out,RZ} = \frac{1}{3}T_3 + \frac{2}{3}T_{RZ} \quad (18)$$

Gas temperature of other zones is calculated according to Eq. 19.

$$T_{out,zone} = T_3 + \eta_{zone} \Delta T_{zone} \quad (19)$$

D. Heat Transfer Calculations

Within a combustor gas temperatures can exceed 2000 K.¹³ When viewed from the durability and structural integrity of the combustor liner and turbine blades, gas and liner temperatures are the most important issues in the preliminary design stage. The heat transfer process between the liner wall and hot gases is shown schematically in Figure 7.

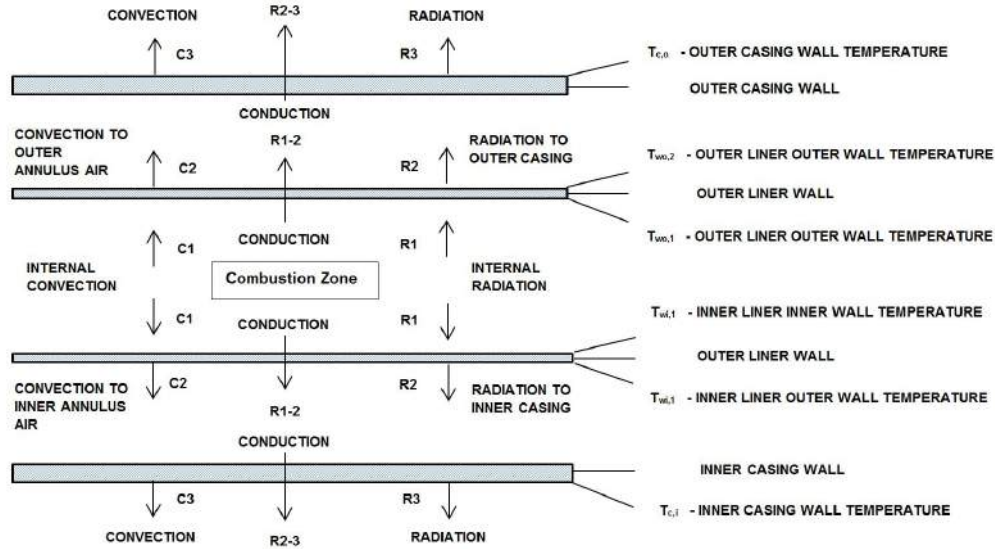


Figure 7: Heat Transfer Schematic Presentation

Heat transfer processes are assumed as steady state conditions and conduction along the liner is assumed to be negligible as per the recommendation of.¹³ The simplified expression for the heat transfer process is,

$$(R_1 + C_1)A_{w1} = (R_2 + C_2)A_{w2} = K_{1-2}A_{wm} \quad (20)$$

Luminous radiation type is considered to predict the radiation effects during heat transfer calculations. Luminous emissivity is mainly a function of the number and size of the solid particles that are related to chemistry, soot formation, atomization quality, fuel distribution, temperature and pressure. Especially, the inlet temperature and liner size are directionally proportional with beam length (l_b) which is the radius of gas hemisphere. Due to the complexity of estimating the luminous emissivity, luminosity factor (L_u) is described by assuming an iso-thermal gas temperature T_g which is surrounded by walls at temperature T_w .¹⁴

Gas emissivity for luminous gases is estimated by the following expression¹³ ;

$$\varepsilon_g = 1 - e^{-290P_3L_u(q_l_b)^{0.5}T_g^{-1.5}} \quad (21)$$

where;

P= gas pressure, kPa

T_g = gas temperature, K

(l_b)= beam length, m

Q = fuel/air ratio by mass

Beam length, l_b is determined with the size and shape of the gas volume as per Eq. 22.¹³

$$l_b = 3.4(\text{volume})/(\text{surface area}) \quad (22)$$

The luminosity factor (L_u) is a mainly function of carbon/hydrogen mass ratios and fuel hydrogen content. For the prediction of L_u , a modified correlation provided by Lefebvre is used.¹³

$$L_u = 336/H^2 \quad (23)$$

Internal radiation flux R_1 from the hot gases into a wall segment is calculated from the equation recommended by Lefebvre as follows¹³:

$$R_1 = 0.5\sigma(1 + \varepsilon_w)\varepsilon_g T_g^{1.5}(T_g^{2.5} - T_{w1}^{2.5}) \quad (24)$$

Given the complexity of reverse flow in the primary zone, flow direction is assumed as straight pipe flow and internal convection C_1 between gas and liner wall is calculated by means of the following formula given by Rizk¹⁵:

$$C_1 = 0.020 \frac{k_g}{D_h^{0.2}} \left(\frac{m_g}{A_L \mu_g} \right)^{0.8} (T_g - T_{w1}) \quad (25)$$

Hydraulic diameter is defined as,

$$D_h = \frac{4A}{P_w} \quad (26)$$

Heat conduction through the liner wall described by:

$$K_{1-2} = \frac{k_w}{t_w}(T_{w1} - T_{w2}) \quad (27)$$

The external radiation flux, using typical emissivity values for both casing and liner walls, can be calculated as follows:

$$R_2 A_w = \frac{\sigma(T_{w2}^4 - T_c^4)}{\frac{(1-\varepsilon_w)}{\varepsilon_w A_w} + \frac{1}{A_w F_{wc}} + \frac{(1-\varepsilon_c)}{\varepsilon_c A_c}} \quad (28)$$

The net radiation heat transfer R_2 from the liner to the annulus air is described as:

$$R_2 = \frac{\sigma \varepsilon_w \varepsilon_c (T_{w2}^4 - T_3^4)}{\varepsilon_c + \varepsilon_w (1 - \varepsilon_c \left(\frac{A_w}{A_c} \right))} \quad (29)$$

External convection C_2 is,

$$C_2 = 0.020 \frac{k_a}{D_{an}^{0.2}} \left(\frac{m_{an}}{A_{an} \mu_a} \right)^{0.8} (T_{w2} - T_3) \quad (30)$$

1. Film Cooling Devices

Film cooling devices are used to protect the liner wall surfaces against high-temperature combustion gases by means of injecting a cold air film.

Combustor chambers are designed to involve a series of cooling slots along the length of the combustion liner to resist the gradual destruction of the film due to the turbulent mixing with combustion gases.¹⁵ Different types of cooling devices are used such as splash cooling rings, wiggle strips, stacked rings, machined rings, z-rings and rolled rings as shown in Figure 8.

In this study, machined ring types are taken into consideration as film cooling devices. Ballal and Lefebvre derived the following statement used for film cooling effectiveness based on turbulent boundary layer models¹⁶.

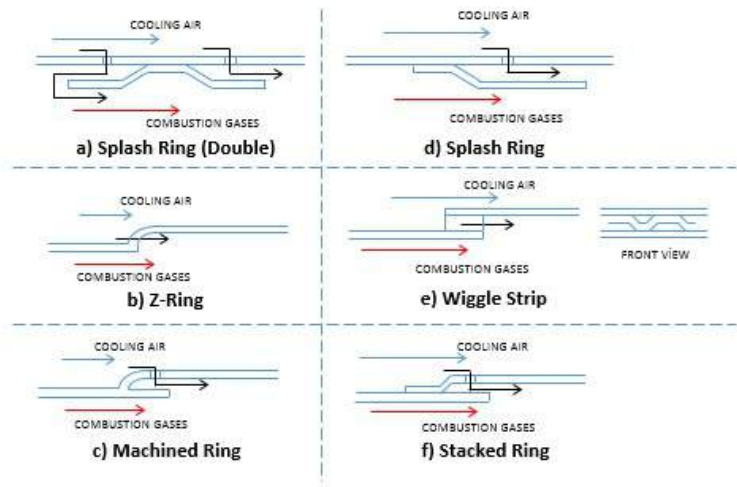


Figure 8: Types of Film Cooling Devices

$$\eta_f = 1.10m^{0.65} \left(\frac{\mu_a}{\mu_g} \right)^{0.15} \left(\frac{x}{s} \right)^{-0.2} \left(\frac{t}{s} \right)^{-0.2} \quad (31)$$

$$\frac{(pV)_a}{(pV)_g} \quad (32)$$

μ is the dynamic viscosity, s is the cooling slot gap, t is the slot thickness and x is the distance downstream of the slot. The subscripts “ a ” and “ g ” denote the air and gas streams, respectively. The film cooling effectiveness is defined as:

$$\eta_f = \frac{T_g - T_{w,ad}}{T_g - T_a} \quad (33)$$

E. Emission Calculations

1. 1-D Network Model

Gas temperature and residence time have a strong effect on NOx production. Therefore, it is assumed that NOx production occurs up until the secondary zone since the highest flame temperature is located between the primary and secondary zones. A semi empirical correlation suggested by Lefebvre¹³ is used to estimate NOx production.

$$NO = 9 \times 10^{-8} P^{1.25} V_c \exp(0.01 T_{st}) / \dot{m} T_{pz} \quad (34)$$

Another correlation presented by Rizk is used for the prediction of CO.¹⁵

$$CO = 10^{(13.477 - 4.5276 \times \log_{10}(T_3))} \quad (35)$$

III. One Dimensional Empirical Network Program

The one dimensional network program was written in a MATLAB environment and consists of a number of functions that are linked to each other. At first, geometrical features of the combustor, initial conditions and some physical constants are defined in the INPUT file. The second function known as FLOWCHECK is the main function of the program and works as an administrator between each function. The data calculated at each function are collected in FLOWCHECK and the required data are distributed to other functions. The remaining functions are FLOWSPLIT, COMBUSTION, ELEMENTS and HEAT TRANSFERS. The FLOWSPLIT performs mass flow rates and pressure drop at each hole. Gas temperatures at each node along the flame tube, combustion efficiency and emission predictions are calculated in the COMBUSTION function. The ELEMENTS file calculates the relevant properties at each node for the heat transfer calculations. Finally, heat transfer along the combustor liner at each node is calculated in the HEAT TRANSFER function. The calculation diagram of the one dimensional empirical network code is illustrated in Figure 9.

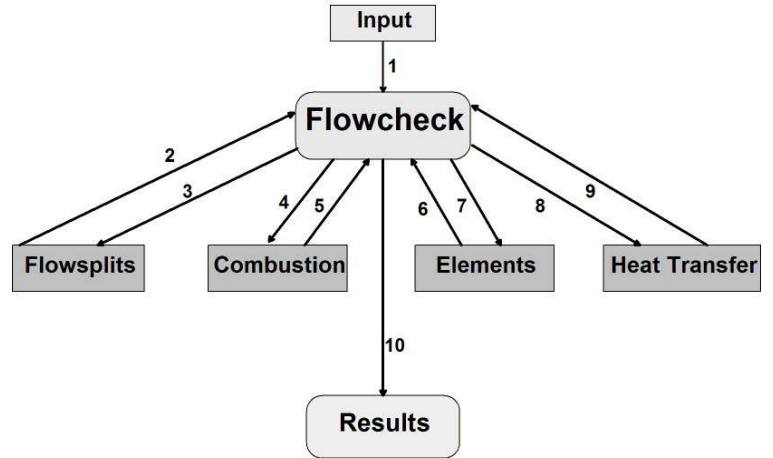


Figure 9: Calculation Flow Chart

IV. Results

Operating conditions for three different regimes and geometric properties of the combustor that are used as input for network calculations are summarized in Table 1, Table 2 and Table 3. As described previously, combustor volume is divided into four zones, namely re-circulation, primary, secondary and dilution zones. Combustor liner is equipped with ten holes including on the inner and outer liner surface. Machined rings are utilized for the film cooling device and plain holes are used for air admitting jets.

Table 1: Operating Condition of the Combustor

	Idle	Cruise	Take-off
Inlet Temperature [K]	396	564	575
Inlet Pressure [kPa]	223	763	802
Total Mass Flow Rate [kg/s]	0.085	0.257	0.266
Overall Air/Fuel Ratio	58.3	46.8	44.5

Table 2: Zone Length

Re-circulation zone [mm]	53.0
Primary zone [mm]	15.0
Secondary zone [mm]	15.4
Dilution zone [mm]	126.6
Total [mm]	210.0

Table 3: Hole Properties

	Inner Hole				
Hole position [mm] (Relative to swirler)	5.10	18.10	38.60	53.10	75.60
Hole type	Machined ring	Plain hole	Machined ring	Plain hole	Machined ring
Number of holes	30	5	30	5	40
Hole diameter [mm]	1.34	3.58	1.39	5.60	1.00
	Outer Hole				
Hole position [mm] (Relative to swirler)	14.30	35.20	44.80	70.40	78.90
Hole type	Machined ring	Plain hole	Machined ring	Plain hole	Machined ring
Number of holes	30	5	40	5	40
Hole diameter [mm]	1.63	3.12	1.70	5.30	1.02

Table 4: Comparison of CFD and 1-D Network Code Results for the Iso-Thermal Case

Hole Type	Hole Type	CFD		1-D Network Code		Error (%)
		Massflow (kg/s)	Mass Fraction (%)	Massflow (kg/s)	Mass Fraction (%)	
	Swirler	0.0392	15.2253	0.0410	15.9160	4.62
Outer Holes	Machined Ring	0.0252	9.8054	0.0212	8.2340	16.00
	Plain Hole	0.0145	5.6467	0.0135	5.2315	7.12
	Machined Ring	0.0210	8.1770	0.0307	11.9245	45.86
	Plain Hole	0.0398	15.4525	0.0387	15.0183	2.70
	Machined Ring	0.0119	4.6096	0.0110	4.2659	7.23
Inner Holes	Machined Ring	0.0197	7.6367	0.0143	5.5644	27.25
	Plain Hole	0.0161	6.2357	0.0177	6.8948	10.28
	Machined Ring	0.0188	7.3081	0.0154	5.9840	18.13
	Plain Hole	0.0379	14.7087	0.0435	16.8506	14.90
	Machined Ring	0.0131	5.0972	0.0106	4.1159	19.21

Table 4 and Table 5 present mass flow distribution and hole discharge coefficients through the film cooling and air jet holes on the inner and outer liners, respectively. To validate the results, 1-D network code results are compared with CFD simulation results for an isothermal case.

Table 5: Comparison of Discharge Coefficients

		Discharge Coefficient	
Hole Type		CFD	1D Network Code
Swirler		0.597	0.625
Outer Holes	Machined Ring	0.714	0.600
	Plain Hole	0.673	0.625
	Machined Ring	0.411	0.600
	Plain Hole	0.642	0.625
	Machined Ring	0.647	0.600
Inner Holes	Machined Ring	0.825	0.600
	Plain Hole	0.567	0.625
	Machined Ring	0.733	0.600
	Plain Hole	0.544	0.625
	Machined Ring	0.743	0.600

Figure 10 shows the prediction of the gas temperature distributions along the combustion chamber at the idle, cruise and take-off regimes. Temperature distributions for inner and outer turn liner walls are also shown in Figure 11a and Figure 11b, respectively. Inconel 635 alloy was considered to be used as the liner material. This alloy is suitable for long-term operations at temperatures up to 1100 K. Figure 11a shows that the predicted liner temperature is 200 K higher than the liner allowable temperature for cruise and take-off conditions.

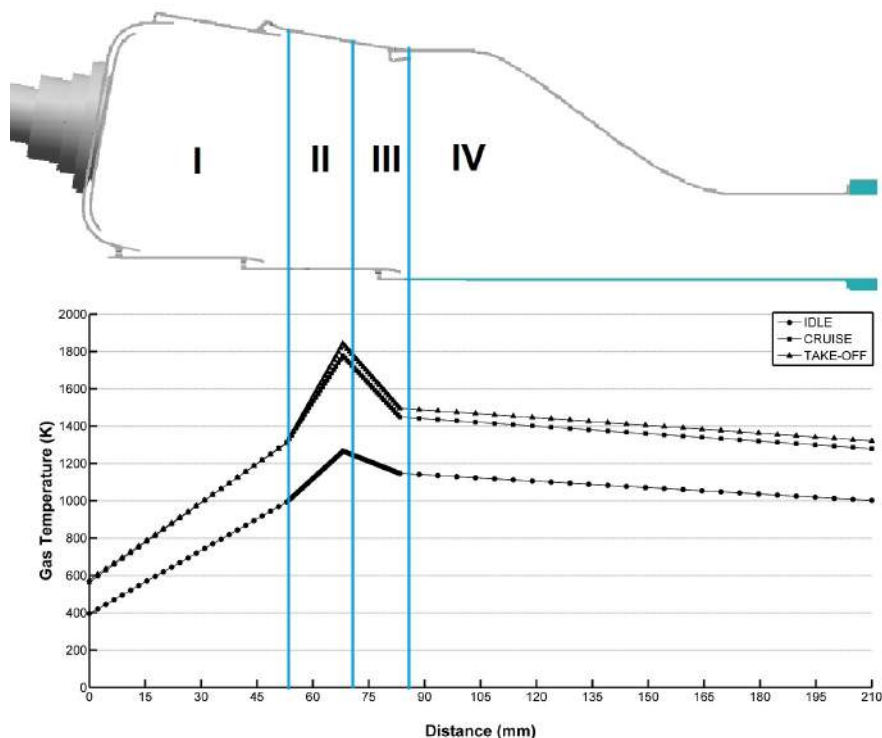
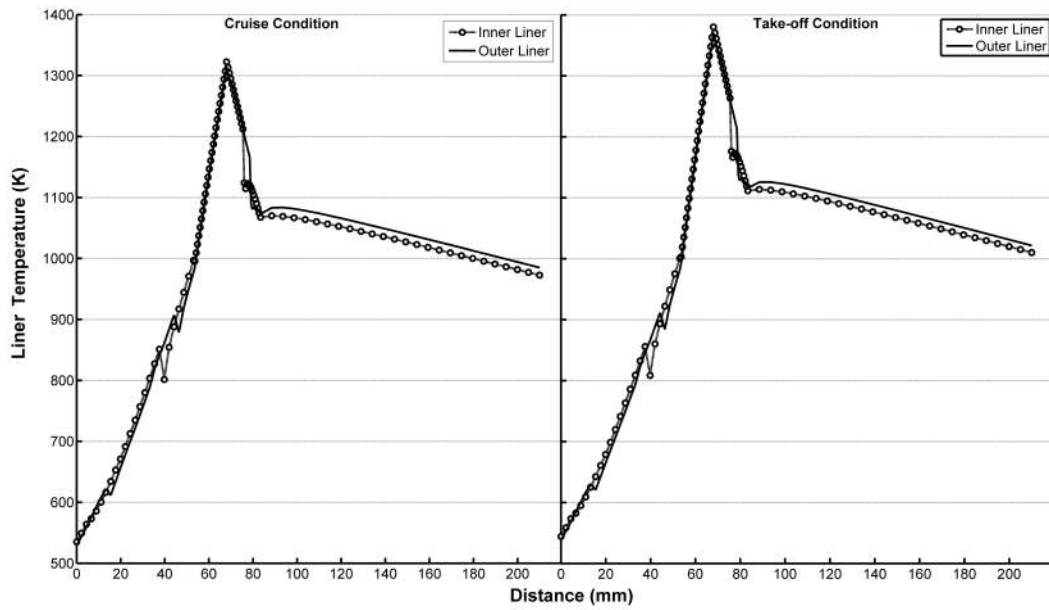
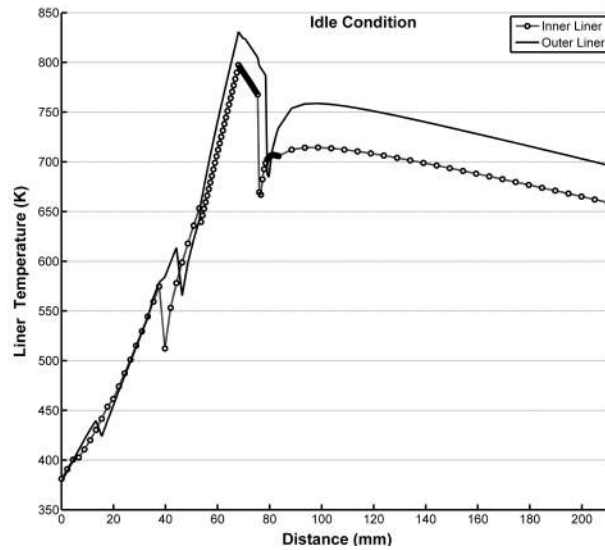


Figure 10: Gas Temperature Distribution (I: Re-circulation Zone, II: Primary Zone, III: Secondary Zone, IV: Dilution Zone)



(a)



(b)

Figure 11: Liner Temperature Distribution

V. Conclusion

A one dimensional network code has been developed to predict mass flow splits, discharge coefficients, overall pressure drops and gas and liner temperatures for a reverse flow combustor. This research provides a useful tool for preliminary design since it enables a quick scan of a multitude of design alternatives prior to detailed CFD simulations and rig experiments. The results showed that overall pressure drop is in an acceptable level for a reverse flow combustor and predicted mass flow splits were similar to numerical simulations. However, the results obtained from this study showed that the predicted liner temperatures were high enough to decrease the strength of liner material. Therefore, some design iteration should be made to achieve lower liner temperatures below 1100 K. Prospective research shall include detailed CFD analyses including reacting turbulent flow simulation in a three dimensional combustor model and shall also incorporate experimental rig tests for liner temperature and discharge coefficient measurements in order to

calibrate and validate the empirical network code approach presented here.

Acknowledgments

Authors would like to gratefully acknowledge funding from the Ministry of Science, Industry and Technology under contract number 009.STZ.2013-1 and also from Istanbul Technical University.

References

- ¹Mongia, H., 1994, "Combustion modelling in design process applications and future direction", AIAA Paper 94-0466
- ²Knight, H.A. and Walker, R.B., 1953, "The component pressure losses in combustion chambers" Aeronautical Research Council R and M 2987, England
- ³Samuel, B.P., 1961, "A Jet Engine Combustor Design Analysis Suitable for Electronic Computers", ASME Paper No. 61-WA-305
- ⁴Joubert, F.M. and Hattingh, H.V., 1982, "Rekenaar-modellering van 'n annulere teenvloei-verbrandingsruim vir gasturbienjins", *Journal of Aeronautical Society*, Vol.3, pp 44-50
- ⁵Dupuis, P., Robert, J.L. and Ouellet, Y., 1987, "A Modified Element Method for Pipe Network Analysis", *Journal of Hydraulic Research*, Vol. 25, No. 1, pp.27-40.
- ⁶Greyvanstein, G.P. and Laurie, D.P., 1994, "A Segregated CFD Approach to Pipe Network Analysis", *International Journal for Numerical Methods in Engineering*, Vol. 37, pp. 3685-3705
- ⁷Stuttaford, P.J., Rubini, P.A., 1996, "Preliminary gas turbine combustor design using a network approach", ASME Paper 96-GT-135
- ⁸Gouws, J.J., 2007, "Combining a One-Dimensional Empirical and Network Solver with CFD to Investigate Possible Modifications to a Commercial Gas Turbine Combustor.", Master Thesis in the Faculty of Mechanical/Aeronautical Engineering of University of Pretoria
- ⁹Norster, E.R., 1980, "Combustor aerodynamics", in Northern Research and Engineering Corporation, "The design and development of gas turbine combustors", Woburn, Massachusetts, Volume 1
- ¹⁰C. Olikara and G. L. Borman, "Calculating Properties of Equilibrium Combustion Products with Some Applications to I.C. Engines", *SAE Paper 750468*, 1975.
- ¹¹Gosselin, P., De Champlain, A., Kretschmer, D., 1999, "Prediction of Wall Heat Transfer for Gas Turbine Combustor", *Journal of Power and Energy*, Vol. 213, pp. 169-180.
- ¹²Odgers, J. and Kretschmer, D., 1980a "Performance evaluation and the Prediction of Pollutant Formation", in Northern Research and Engineering Corporation, "The Design and Development of Gas Turbine Combustors", Woburn, Massachusetts, USA, Volume 2.
- ¹³Lefebvre, A.H., 1988, "Gas Turbine Combustion" Second Edition, Taylor and Francis.
- ¹⁴Lienhard IV, J.H., and Lienhard V, J.H., 2003, "The heat transfer textbook - Third Edition", Phlogiston Press, Cambridge Massachusetts.
- ¹⁵Rizk, N.K., 1994, "A Quasi-3D Calculation Method for Gas Turbine Combustor Liner Wall Cooling Techniques", ASME Paper No. 94-GT-316.
- ¹⁶Ballal, D.R. and Lefebvre, A.H., 1986, "A Proposed Method for Calculating Film-cooled Wall Temperatures in Gas Turbine Combustion Chambers", ASME Paper No. 72-WA/HT-24.
- ¹⁷Heywood, J.B. and T. Mikus, 1973 "Parameter Controlling Nitric Oxide Emissions From Gas Turbine Combustors", in AGARD Propulsion and Energetic Panel 41st Meeting on Atmospheric Pollution by Aircraft Engines. London.
- ¹⁸Zel'dovich Y, Sadovnikov P, Frank-Kamenetskii D., 1947 "Oxydation of nitrogen in combustion", Tech. Rep. Moscow: Academy of Sciences of the USSR.
- ¹⁹Dodds, W.J., and Bahr, D.W., 1990, "Combustion System Design", in A.M. Mellor, ed., "Design of Modern Gas Turbine Combustors", pp 343-476, Academic Press, San Diego.
- ²⁰Odgers, J. and Kretschmer, D., 1980b "Basic Design Method - Can Combustors", in Northern Research and Engineering Corporation, "The Design and Development of Gas Turbine Combustors", Woburn, Massachusetts, USA, Volume 2.